A Strategy to Adjust Anode Vertical Position After Setting Using Anode Current Profile

Choon-Jie Wong[1], Jie Bao[2], Maria Skyllas-Kazacos[3], Barry Welch[4], Nadia Ahli[5], Amal Aljasmi[6] and Mohamed Mahmoud[7]

1. Postdoctoral Fellow
2. Professor
3, 4. Emeritus Professor
University of New South Wales, Sydney, Australia
5. Senior Manager
6, 7. Manager
Emirates Global Aluminium, Dubai, U.A.E.

Corresponding author: j.bao@unsw.edu.au
https://doi.org/10.71659/icsoba2024-al046

Abstract

Anode change events introduce significant mass and thermal disturbances to the aluminium reduction process. Smelters aim to mitigate these impacts by setting new anodes at a higher vertical position to accommodate reduced carbon consumption, ensuring that once the new anodes recover their normal current load, their bottom surface aligns with other anodes. However, this increment may not be optimally implemented due to varying local cell conditions and work practice tolerance. Continuous measurements from an Individual Anode Current Monitoring system facilitates the prediction of anode consumption rates and variations in anode-cathode distance following anode changes. This paper proposes re-adjusting the vertical position of new anodes based on the anode current recovery profile, aiming to minimise unnecessary crane usage. Prompt restoration of anode current distribution aids in mitigating process perturbations from subsequent anode change events, thereby enhancing cell stability and energy and operational efficiency.

Keywords: Anode setting, Individual anode current measurement, Mass and energy balances.

1. Introduction

In the Hall-Héroult process, aluminium is produced by the reduction of alumina and the oxidation of carbon anodes. The anodes are consumed continuously and must be replaced manually at the end of their service life, typically around 3–4 weeks. At this point, the anodes having diminished to no less than a quarter of their original size to prevent the iron stubs from being chemically attacked by the corrosive electrolytic bath, which would lead to product contamination [1]. Anode changes or “settings” are staggered (see Figure 1) for practicality and to maintain process continuity, as these changes significantly disrupts the cell mass and thermal balances.

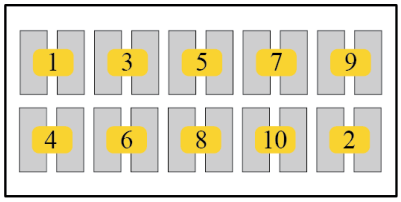

Figure 1. Example sequence of anode pair replacements in a cell.

Consequently, each cell in the pot room undergoes an anode change every few days, making this the most common manual operation. Given the regularity of the operation and the disturbance

caused, an optimal anode change strategy and its proper execution are critical for maintaining high cell efficiency. This includes re-adjustment of the anode vertical position, and consequently local ACD, post-change where necessary.

A common strategy to determine if re-adjustment is necessary involves measuring the instantaneous current flowing through the anode rod using a hand-held tool to ensure it falls within acceptable bands. However, this method assumes a well-operating, homogeneous cell with the newly changed anodes being the sole irregularity. In actuality, the re-distribution of anode current is not limited to local anode condition, as it could be caused by elsewhere in the cell. This assumption is increasingly challenged in modern cells, where the growing global aluminium demand has led to capacity increase in existing smelters and the construction of larger cells with more anodes, higher line currents, squeezing anode-cathode distance (ACD), and a larger anode-to-electrolyte volume ratio [2-4]. These factors exacerbate the non-uniformity in alumina concentrations and ACDs, among other spatial cell conditions. Consequently, as modern cells operate closer to process constraints, non-uniformity in anode current distribution, heat generation, and consumption of alumina and anodes are not uncommon. Thus, spot anode current measurements provide insufficient information to accurately determine the need for re-adjusting the vertical position of anodes previously set.

Continuous measurement and analysis of anode currents have garnered significant interest due to their potential in revealing spatial information on cell conditions. Continuous individual anode currents can optimise alumina feeding strategies [5-13], detect early signs of process abnormalities [14-19], and improve cell operation strategies [20-22]. Aligning with the Industry 4.0 vision of using advanced sensors for digital automation, control, analytics, and flexible manufacturing, our team has developed sophisticated measurement systems that provide real-time data on individual anode currents. These data enable strategies that ensure the energy-intensive smelting process remains adaptable and efficient, such as power modulation strategies to adjust electrical power usage in smelters in response to a variable power landscape driven by decarbonisation efforts and increased integration of intermittent solar energy [23-26]. This paper explores another application of continuous anode current measurement: using anode current profile of new anodes to determine if their vertical positions can be improved post-change.

2. Anode Change and Vertical Position Increment

The operation begins with crust breaking to release the anodes, during which the crust and anode cover material fall into the bath, introducing a thermal energy deficit and an excess of alumina. Next, the spent anode butt is removed, taking with it at least 50 kWh of stored energy. The replacement anode, typically at pot room temperature (far below the bath liquidus temperature), causes the surrounding bath to rapidly solidify. This solid phase, having a different composition from the liquid bath, alters the bath composition. Additionally, the solid phase impedes bath flow, slows mass transport, and introduces spatial variations. Furthermore, this freeze acts as an electrical insulator, blocking and redistributing anode current to other anodes. At least 160 kWh are needed to restore optimal cell conditions, including the dissolution of the freeze and heating the bath and new anodes to operating temperatures. Although preheating anodes can reduce these impacts, it is not commonly practiced due to higher energy costs [27].

Initially, the freeze completely covers the anode in contact with the bath, preventing current flow. Anode current gradually increases to its operating capacity as the freeze dissolves over hours or days, during which local heat generation and material consumption are relatively less than that of other anodes. Consequently, informed by positive experimental results [28, 29], smelters typically set the new anode at a greater vertical position than the old butt it replaces, ensuring the ACD of the new anode matches that of other anodes when it eventually draws the normal current load.

Figure 2 presents simulation results for a 36-anode cell using an anode change model published in our previous work [30]. The figure demonstrates the effects on current profiles for recently set anodes and existing anodes when the new anodes are positioned too low, at the optimal height, or too high. The 32-hour mark is indicated on the diagram, representing the time by which the cell must stabilise before the next anode pair is scheduled for replacement. The simulation results also reveal that when the current from the two recently set anodes is evenly redistributed among the remaining 34 anodes, the anode currents for the older anodes exhibit minimal variation. However, an uneven distribution can result in some anodes experiencing higher current densities, which may lead to the onset of anode effects if sustained.

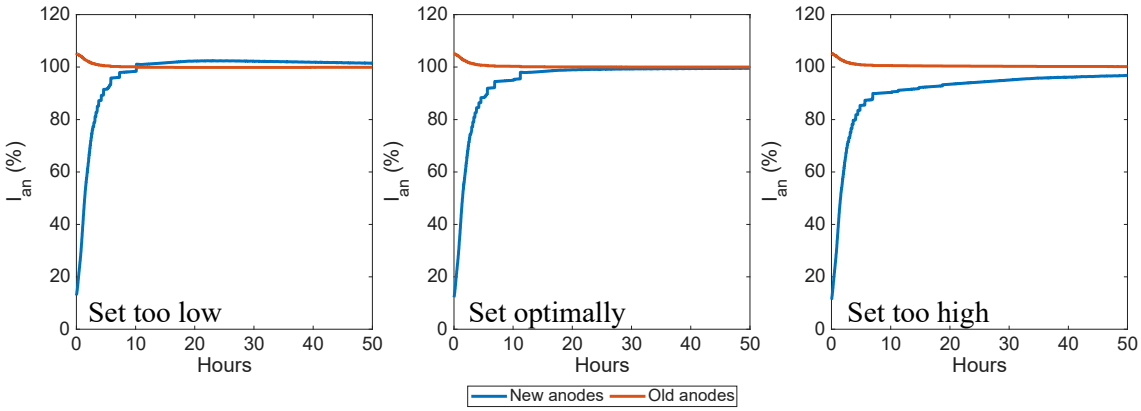

Figure 2. Anode current profiles for various anode vertical positions.

The vertical position increment for anode change significantly affects cell efficiency, as anodes set too high result in:

- A higher local ACD, resulting in a higher bath resistance in the vicinity.
- Anode current to preferentially re-distribute to other anodes with lower path resistances.
- Decreased heat generation in the area, which is proportional to the square of current.
- Slower freeze dissolution and slower anode current recovery rate.
- After freeze dissolution, local ACD is still higher than target value. This causes poor anode current distribution leading to variability in spatial conditions.

Conversely, anodes set too low result in:

- A lower local ACD, lowering the local bath resistance.
- Anode current preferentially flows through this anode with the relatively lower electrical path resistance.
- While this initially generates more heat conducive to freeze dissolution, the local ACD is lower than target value after the freeze is dissolved. This causes poor anode current distribution, variability in spatial conditions, and increases the risk of electrical shorting with the rolling metal pad.

However, implementing this vertical position increment accurately is challenging due to the practical difficulties of precisely manoeuvring anodes that weigh around 20 tonnes. Moreover, while a constant vertical position increment is applied for operational simplicity, the optimum increment depends on and affects anode current as well as local mass and thermal balances, influenced by factors such as:

- Temperature and electrical resistance of the anode assembly (including rod, transition join, stub, thimble, and carbon), bath, and cathode.
- Thermal conduction of anode assembly, bath, cathode, anode dressing material, and crust.

- Thermal convection due to bath flow, fume extraction, outflow of hot gases, and inflow of cool air through crevices, open doors, and shields.
- Thermal radiation and other heat losses due to cell design and configuration, anode replacement cycle pattern, anode location in the cell, heat emitted by neighbouring cells, seasonality, and weather conditions.

Given the impracticality of ensuring the implemented position increment is optimal, we focus on correcting the position where necessary.

3. Individual Anode Currents

While the line current flowing through the cells is regulated by rectifier systems, within a cell it is distributed among the anodes, which are electrically connected in a parallel network. This distribution is influenced by the local impedances of each anode-cathode path, arising from factors such as bath composition, ACD, bubbles, and anode freeze [31]. Consequently, measuring individual anode currents reveals spatial variations within the cell, enabling a more precise understanding of cell dynamics. This approach has several applications, including the optimisation of alumina feeding by identifying areas of low alumina concentration, early detection and intervention of process abnormalities such as anode effect onset and feeder faults, and the development of model-based and data-based soft sensors and controllers.

Many smelters aim to operate cells with a uniform anode current distribution. Since current is the driving force of electrochemical processes, an even current distribution ensures consistent material consumption rates and heat generation rates throughout the cell. Empirical data [32] links uniform current distribution to higher cell efficiency. Anode current and ACD exhibit self-stabilising dynamics — Given sufficient time, the anode current distribution can equalise through increased carbon consumption if the local ACD is relatively low. However, in practice, this equalisation may be hindered by the frequency of anode change operations and the resulting alterations in the shape of the metal pad.

We have developed, and published elsewhere [33], a measurement system that offers real-time monitoring of individual anode currents. The system employs smart sensors daisy-chained on a common bus for digital data transfer (see Figure 3), which limits electromagnetic interferences and can provide self-configuration and self-diagnosis capabilities, ensuring ease of maintenance and robustness. Each sensor contains a microprocessor for distributed signal processing, including ‘oversampling and decimation’ [34] to increase effective sampling resolution, signal amplification, and signal filtering. This smart digital system samples signals from the anode beam, allowing uninterrupted data collection even during various cell operations, including anode changes.

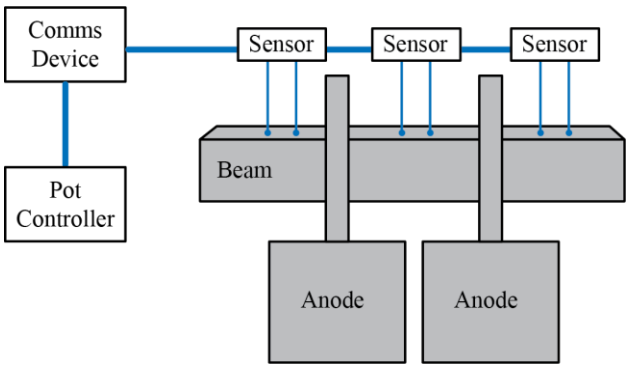

Figure 3. Sensor measures anode currents from the beam, ensuring signal continuity through anode changes.

4. Strategy to Re-Adjust Vertical Position of New Anodes with Limited Crane Resources

During anode replacement, a 'pot tending machine' equipped with a crane and trolley manoeuvres the anodes. This overhead crane is fitted with various electro-hydro-mechanical systems to perform multiple routines, including crust breaking, anode dressing, fluoride feed hopper refilling, metal tapping and pouring, bath tapping and pouring, and lifting tasks in the pot room, such as handling the anode beam, cell structure, and crucible during installation, operation, maintenance, and cleaning. Given its multi-purpose role, the crane operates on an extremely tight schedule, running almost continuously. One crane is expected to service 35 cells on average [35], and the operation team uses it around the clock in the pot room, with any brief downtime reserved for process upset corrections and scheduled preventative maintenance [36].

Crane availability is crucial for efficient pot line operation, and two closely monitored metrics in many smelters are crane utilisation and reliability [37]. For instance, one smelter identified crane unavailability as a contributing factor to falling current and energy efficiencies [38]. Another smelter identified crane shortages as their primary cause of cell operation disruptions and subsequently increased their metal tapping cycle from 32 to 48 hours to reduce backlogs and provide adequate time for maintenance [39]. For larger cells with more anodes, the crane utilisation rate may be more constrained.

Theoretically, the fastest anode freeze dissolution and quickest cell disturbance rejection can be achieved via PID-style control of anode vertical position. Initially, anodes are set with a low position increment or even a slight decrement, providing a path with lower electrical resistance conducive to quick anode warming and faster recovery of nominal anode current. As anode current approaches or reaches the target value, the anodes are raised to match the ACD of other anodes. However, since most cells lack individual anode drive systems, this approach requires scheduling additional time for new events, straining the already limited crane resources. Therefore, minimising crane usage where possible is an important objective when developing strategies to re-adjust the vertical position of anodes after setting.

Hence, a more practical strategy is as follows:

1. Set the anodes according to the standard operating procedure, with a vertical position increment that is practiced in the smelter.
2. Continuously monitor and record the anode current distribution.
3. Calculate anode consumption and/or ACD as needed from the history of anode current distribution (this will be covered in the next section).
4. Before the next scheduled anode change operation, calculate the needed vertical position adjustment (this will be covered in the next section).
5. If the required adjustment exceeds the work practice tolerance (*e.g.*, finer than 3 mm), it can be omitted because the practice cannot achieve such precision. Otherwise, perform the adjustment.
6. Continue the next anode change operation. Repeat from 1.

Coinciding position readjustment activities with the setting of the next anode pair has the benefit of allowing the anode freeze sufficient time to dissolve and the cell to stabilise. It also takes advantage of the crane's proximity, requiring minimal additional lateral movement, as illustrated in Figure 4. This strategy eliminates the need to schedule extra events and reduces the time associated with long crane travel. The pot monitoring system, which receives real-time anode current data, can automatically calculate and suggest any necessary vertical position adjustments. This approach cuts down on labour time and ensures that adjustments are made only for significant vertical position errors, thereby minimising crane usage.

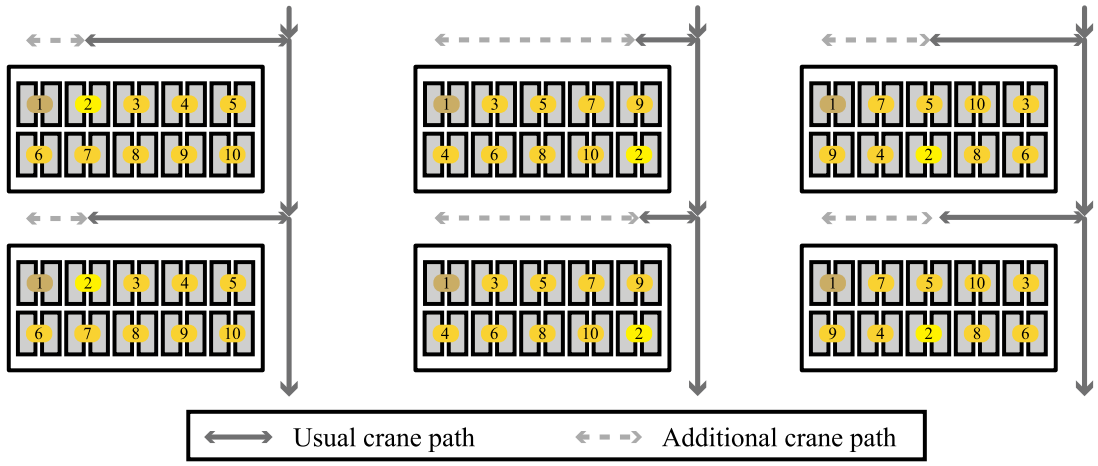

Figure 4. Proposed schedule minimises crane time and movement regardless of sequence. Anode pair 1 was last set, and anode pair 2 will be changed next.

5. Determining Vertical Position Adjustment

5.1 Method 1: Using Model-Based Soft Sensor

We have published a study elsewhere [40] on a soft sensor designed to estimate key smelting process variables following anode change operations. This soft sensor functions as a state estimator, utilising a discretised mass and thermal balance model to describe the real-time consumption of anodes and dissolution of anode freeze.

Figure 5 illustrates the outputs from the soft sensor running on data collected from an industrial smelter. The sensor takes cell control actions, continuous measurements of individual anode currents, and cell voltage as inputs. Shortly after an anode change, the soft sensor begins estimating various cell conditions, including temperature variations, the ACD of new and older anodes, and the extent of anode freeze dissolution expressed as the percentage of effective anode area. The figure shows that the anode freeze has melted by 10 hours, but the ACD of the recently set anodes remains high.

Vertical position adjustment of the anodes is scheduled at 15 hours. The difference between the estimated ACDs of the new and remaining anodes is used to compute the necessary vertical position adjustments. Before implementing these adjustments, the model allows for simulations to predict the outcomes, enabling verification that the anode current distribution changes as intended. Figure 5 demonstrates this capability, showing predictions under base feeding rates plotted with dashed lines. The predictive capability of the model not only improves the precision of anode position adjustments but also enhances overall process efficiency and stability.

Vertical position adjustment of the anodes is scheduled at 15 hours. The difference between the estimated ACDs of the new and remaining anodes is used to compute the necessary vertical position adjustments. Before implementing adjustments, the model also allows simulations to predict the outcome, enabling verification that the anode current distribution changes as intended. Figure 5 demonstrates this capability, showing predictions under base feeding rates plotted with dashed lines. The predictive capability of the model not only improves the accuracy of anode position adjustment calculations but also enhances overall process efficiency and stability.

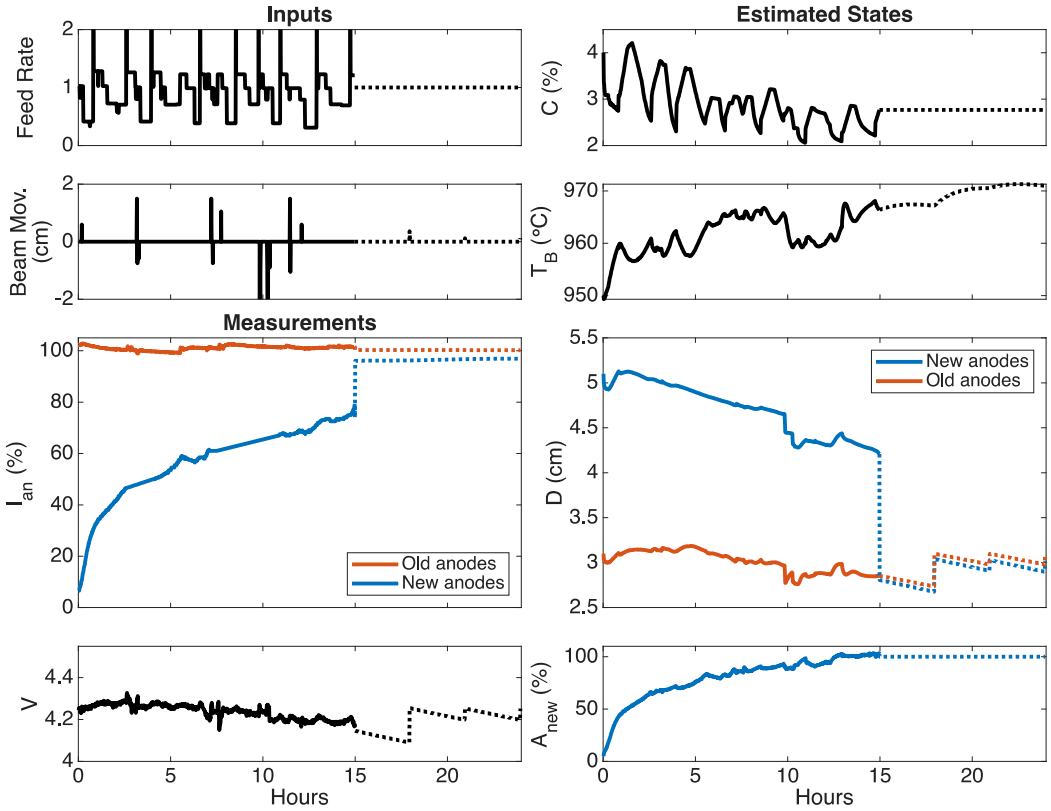

Figure 5. Soft sensor used to estimate past states and predict future steps. C is alumina concentration, T_B is bath temperature, D is ACD, and A_{new} is effective anode area.

5.2 Method 2: Using Simple Anode Consumption Model

While the first method is expected to provide robust and accurate results, it requires system identification and estimator tuning to ensure accurate measurements and timely convergence. Not all smelters may have access to the resources needed to develop a well-performing soft sensor. Therefore, we discuss a more accessible method using a simple anode consumption model.

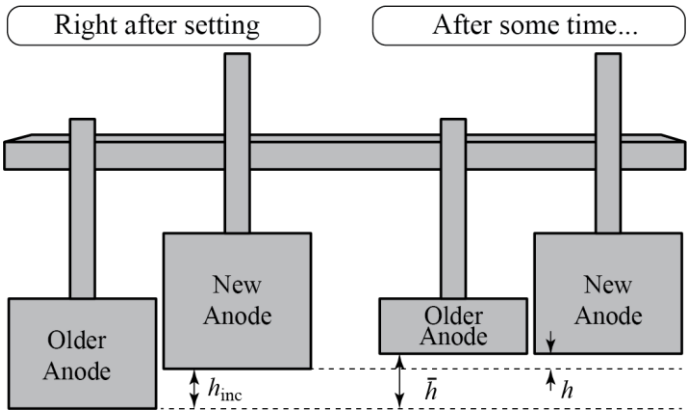

Figure 6. Different carbon consumption rates.

New anodes are set at a higher vertical position to accommodate reduced carbon consumption after anode change. This is so after the new anodes recover their normal current load, their bottom surface area would be at the same vertical position as other anodes (see Figure 6):

$$(h_{\text{inc}} + e) + h(t) = \bar{h}(t) \tag{1}$$

where:

h_{inc} Vertical position increment when setting the new anodes according to work practices, cm
e Error in vertical position increment if height mismatches, cm
h Height reduction of a new anode at time t since last anode change t_0, cm
$\bar{h}$ Mean height reduction of other anodes at time t since anode change t_0, cm

The mean rate of anode height reduction due to consumption can be measured empirically. While this is a cell design parameter, measuring the butt height of anode from various stall locations across many cells over multiple anode change cycles will account for variances from cell age, cell condition, and anode quality:

$$\bar{h}(t) = \frac{H_{\text{new}} - H_{\text{butt}}}{t_{\text{cycle}}} \cdot t \tag{2}$$

where:

H_{new} Mean height of new anode, cm
H_{butt} Mean height of anode butt, cm
t_{cycle} Anode service life, s

Anode height reduction is primarily caused by carbon gasification at the electrode-electrolyte interface. Table 1 summarises the two main electrochemical half reactions involved with varying selectivity, along with parameter z to be used in Faraday's Law of Electrolysis. A small amount of carbon (< 5 %) also detaches as particulates due to bath agitation. The height reduction of an anode between any two times t_0 and t_1 is:

$$h = \int_{t_0}^{t_1} \dot{h}(t)\ \mathrm{d}t = \int_{t_0}^{t_1} \left(\frac{M}{Fz} \frac{\eta(t) I_{\text{an}}(t)}{A(t)\rho(t)} + \frac{\dot{m}_{\text{dust}}}{A(t)\rho(t)} \right) \mathrm{d}t \tag{3}$$

where:

$\dot{h}$ Rate of decrease in anode height, cm/s
M Atomic mass of carbon, 12 g/mol
F Faraday constant, 96 485 C/mol
z Weighted number of charges involved in the reaction, 3.6
η Current efficiency of the cell, ratio
I_{an} Current flowing through this anode, A
A Bottom surface area of anode, cm^2
ρ Apparent density of anode, g/cm^3
$\dot{m}_{\text{dust}}$ Rate of carbon particle detachment, g/s

Table 1. Equivalent charges transferred in carbon consumption reactions.

Half-cell reaction		Selectivity	z
$C + 2O^{2-} = CO_2 + 4e^-$	(4)	80-85 %	4
$C + O^{2-} = CO + 2e^-$	(5)	15-20 %	2
Equivalent overall reaction (weighted mean)		100 %	3.6

In practice, anode current is obtained as a time-series data and not as an explicit function of time. Therefore, instead of performing analytical integration, Riemann summation over discrete time periods is applied to Equation 3:

$$h = \int_{t_0}^{t_1} \dot{h}(t)\ \mathrm{d}t \approx \sum_{i=0}^{n-1} \left(\frac{M}{Fz} \frac{\eta_i I_{\text{an},i}}{A_i \rho_i} + \frac{\dot{m}_{\text{dust}}}{A_i \rho_i} \right) \Delta t \tag{6}$$

where:

Δt Sampling time of anode currents, s
n Number of time segments, given by $\frac{t_1 - t_0}{\Delta t}$
i i-th time segment

The parameters in Equation 6 can be verified by choosing t_0 to be the setting time of an anode and t_1 to be the setting time of the same anode one service cycle later, such that $t_1 - t_0 = t_{\text{cycle}}$. The calculated height reduction h should be equal to the empirical measurement $(H_{\text{new}} - H_{\text{butt}})$. Once validated, this equation can be used in Equation 1 by choosing t_0 to be the time of last anode change and t_1 to be the current time, such that the computed value of h gives the anode height reduced since last anode change.

Alternatively, the anode height reduced since last anode change can be approximated. Current recovery of a new anode happens over a short time relative to the service life of the anode, and so it may be approximated that the mean height consumption rate occurs at full anode current load. Therefore, the reduced height consumption during current pickup can be determined by the ratio of the integral of the actual anode current over a given time period to the integral of the mean anode current load over the same period, Equation 7:

$$h \approx \frac{\sum_{i=0}^{n-1}(I_{\text{an},i}\,\Delta t)}{\sum_{i=0}^{n-1}(\overline{I_{an}}\,\Delta t)} \cdot \bar{h} = \frac{\sum_{i=0}^{n-1} I_{\text{an},i}}{n\overline{I_{an}}} \cdot \frac{H_{\text{new}} - H_{\text{butt}}}{t_{\text{cycle}}} \cdot (t_1 - t_0) \tag{7}$$

where:

$\overline{I_{an}}$ Mean anode current load, given by line current divided by number of anodes, A

t_0, t_1 Time of last anode change and current time, s. For $(t_1 - t_0) \ll t_{\text{cycle}}$.

Finally, substituting Equations 2 and 7 into Equation 1, the required corrective vertical height adjustment is:

$$e \approx \frac{H_{\text{new}} - H_{\text{butt}}}{t_{\text{cycle}}}(t_1 - t_0)\left[1 - \frac{\sum_{i=0}^{n-1} I_{\text{an},i}}{n\overline{I_{an}}}\right] - h_{\text{inc}} \tag{8}$$

This required adjustment is rounded off to the nearest 0.1 cm and only implemented if it is within work practice tolerance (*e.g.*, more than 0.3 cm):

$$u(e) = \begin{cases} 0.1\ \text{round}(10e), & |e| > 0.3\ \text{cm} \\ 0, & \text{otherwise} \end{cases} \tag{8}$$

where:

u Vertical height adjustment to be implemented (positive means raising and vice versa), cm.

Figure 7 illustrates the application of the algorithm through a simulation. To better demonstrate the relationship between the states, noise was not incorporated into the model. An anode pair was replaced at 0 hours, with the next anode pair replacement scheduled for 32 hours. This will coincide with any necessary vertical position adjustments, allowing sufficient time for the freeze to dissolve and the cell to stabilise.

The simulation shows that the ACD of the newly changed anode pair initially decreases rapidly. This is due to the low carbon consumption at low anode current, combined with the accumulation of aluminium at the bottom of the cell, which reduces the ACD. However, as the current recovers, carbon consumption increases, causing the ACD of the recently set anodes to converge more slowly to the mean ACD of the cell. The pot controller, using the anode current profile, reaches the same conclusion. By applying Equations 1–8, a vertical position adjustment value is recommended to the operations team, who then implement the adjustment. Figure 7 shows that post-adjustment, the anode current has achieved increased uniformity. This uniformity is expected to enhance the current efficiency of the cell.

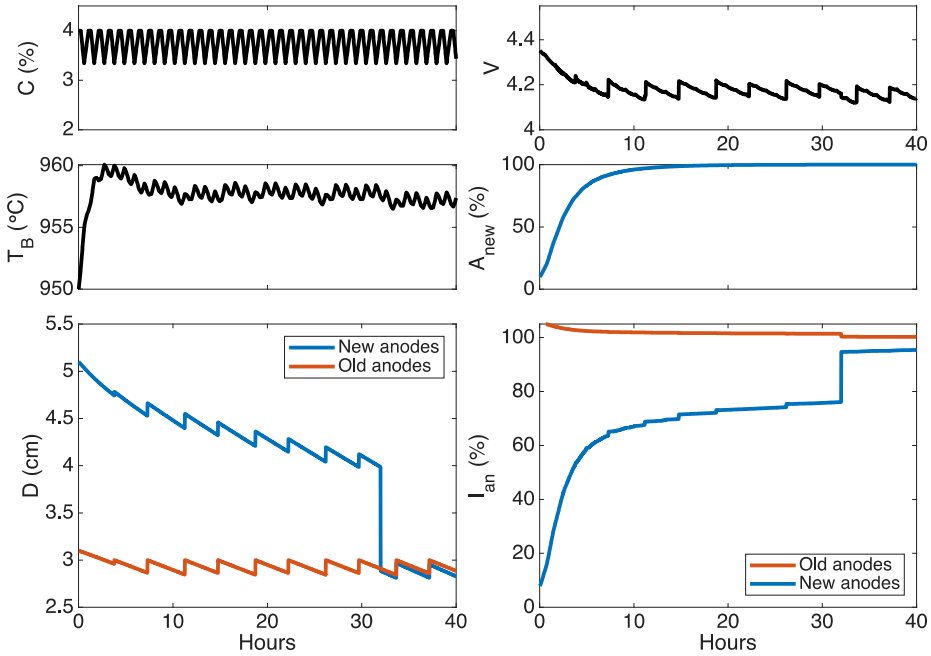

Figure 7. Algorithm used to calculate required vertical position adjustments.

6. Conclusions

Traditionally, some smelters determine the need for re-adjusting the vertical position of recently set anodes based on spot anode current measurements. This paper proposes enhancing the accuracy of this decision by incorporating the history of anode current recovery to full load after setting.

Two methods are presented. The first method employs a soft sensor, based on a mass and thermal balance model that accounts for anode consumption and freeze dissolution, to estimate crucial process variables such as local ACDs and the extent of anode freeze dissolution. This sensor also supports predictive modelling to verify intended changes in anode current distribution, thereby increasing operator confidence and allowing for result validation after adjustments have been implemented. The second method, a simpler anode consumption model, offers an accessible alternative for smelters with limited resources. This model utilises Faraday's Law of Electrolysis to incorporate the rate of carbon consumption for determining necessary anode position adjustments. Both methods aim to achieve a more uniform current distribution, improving material consumption rates and heat generation consistency across the cell. This uniformity is expected to enhance both current efficiency and energy efficiency, ultimately contributing to more efficient aluminium production. However, it is noted that an even ACD does not guarantee a perfectly even anode current distribution, which also depends on other factors such as anode age.

Future work includes careful planning for industrial testing and implementation to isolate and measure the positive impact on current efficiency. Additionally, further research should investigate the effects of anode current distribution on reaction rates, focusing on avoiding anode effects, excessive overpotentials, and perfluorocarbon (PFC) generation.

7. Acknowledgement

The authors gratefully acknowledge the financial support provided by the ARC Research Hub for Integrated Energy Storage Solutions (IH180100020). We also extend our sincere thanks to

Emirates Global Aluminium Jebel Ali Operations for their invaluable technical support, particularly the Technology Development and Transfer team and the Operations team.

8. References

1. Kai Grjotheim and Halvor Kvande, *Introduction to aluminium electrolysis: Understanding the Hall-Heroult process*, 2nd Edition, Dusseldorf, Aluminium-Verlag, 1993, 260 pages.
2. Marc Dupuis and Barry J. Welch, Designing cells for the future – Wider and/or even higher amperage?, *ALUMINIUM*, (2017), 45-49.
3. Alton Tabereaux, Super-high amperage prebake cell technologies in operation at worldwide aluminum smelters, *Light Metals Age*, Vol. 75, No. 1, (2017), 26-29.
4. David Wong et al., Latest progress in IPCC methodology for estimating the extend of PFC greenhouse gases co-evolved in the aluminium reduction cells and challenges in reducing these emissions, *Proceedings of the 37th International ICSOBA Conference*, Krasnoyarsk, Russia, 16–20 September 2019, *TRAVAUX* 48, 735-758.
5. Stig Rune Jakobsen et al., Estimating alumina concentration distribution in aluminium electrolysis cells, *IFAC Proceedings Volumes*, Vol. 34, No. 18, (2001), 303-308.
6. Kristin Hestetun and Morten Hovd, Detecting abnormal feed rate in aluminium electrolysis using extended Kalman filter, *IFAC Proceedings Volumes*, Vol. 38, No. 1, (2005), 85-90.
7. Yuchen Yao et al., Monitoring local alumina dissolution in aluminum reduction cells using state estimation, *Light Metals* 2015, 577-581.
8. Yuchen Yao et al., Method for estimating dynamic state variables in an electrolytic cell suitable for the Hall-Heroult electrolysis process, *Patent WO 2017/141134 A1*, filed August 2017.
9. Yuchen Yao and Jie Bao, State and parameter estimation in Hall-Heroult cells using iterated extended Kalman filter, *IFAC-PapersOnLine*, Vol. 51, No. 21, (2018), 36-41.
10. Jing Shi et al., Multivariable Feeding Control of Aluminum Reduction Process Using Individual Anode Current Measurement, *IFAC-PapersOnLine*, Vol. 53, No. 2, (2020), 11907-11912.
11. Jing Shi et al., A New Control Strategy for the Aluminum Reduction Process Using Economic Model Predictive Control, *IFAC-PapersOnLine*, Vol. 54, No. 11, (2021), 49-54.
12. Jing Shi et al., Advanced Model-Based Estimation and Control of Alumina Concentration in an Aluminum Reduction Cell, *JOM*, Vol. 74, No. 2, (2022), 706-717.
13. Jing Shi et al., Advanced Monitoring and Control of Alumina Concentration in Aluminum Smelting Cells, *IFAC-PapersOnLine*, Vol. 56, No. 2, (2023), 6194-6199.
14. Ruoyu Huang, Zetao Li, and Bin Cao, Design and Implementation of Online Detection System for Anode Current Distribution in Aluminum Reduction Cell, *China Automation Congress (CAC)*, 2021, 5652-5657.
15. Iliya I. Puzanov et al., Continuous monitoring of information on anode current distribution as means of improving the process of controlling and forecasting process disturbances, *Journal of Siberian Federal University. Engineering & Technologies*, Vol. 9, No. 6, (2016), 788.
16. Cheuk-Yi Cheung et al., Characterization of individual anode current signals in aluminum reduction cells, *Industrial & Engineering Chemistry Research*, Vol. 52, No. 28, (2013), 9632-9644.
17. Jeffrey T. Keniry et al., Digital processing of anode current signals: an opportunity for improved cell diagnosis and control, *Light Metals* 2001, 1225-1232.
18. R. Hvidsten and K. Rye, Practical Applications of the Continuous Measurement of Individual Anode Currents in Hall-Heroult Cells, *Light Metals* 2008, 329-331.
19. Valdis Bojarevics and James W. Evans, Mathematical modelling of Hall-Heroult pot instability and verification by measurements of anode current distribution, *Light Metals* 2015, 783-788.

20. Ali Jassim, *Use of individual anode current monitoring to optimise work practices, priorities and fault detection to minimize energy consumption and perfluorocarbons*, PhD Thesis, University of New South Wales, Sydney, Australia, 2016.
21. Shuai Yang et al., Online anode current signal in aluminum reduction cells: measurements and prospects, *JOM*, Vol. 68, No. 2, (2016), 623-634.
22. James W. Evans and Nobuo Urata, Technical and operational benefits of individual anode current monitor, *Proceedings of 10th Australasian Aluminium Smelting Technology Conference*, Launceston, Tasmania, Australia, 2011, Paper 4a2.
23. Choon-Jie Wong et al., Studies on Power Modulation of Aluminum Smelting Cells Based on a Discretized Mass and Thermal Dynamic Model, *Metallurgical and Materials Transactions B*, Vol. 54, (2023), 1-16.
24. Till Reek, *Power Modulation of aluminium Reduction Cells — Operational Constraints and Process Limits*, PhD Thesis, University of New South Wales, Sydney, Australia, 2015.
25. Choon-Jie Wong et al., A Study on Predicting Electrolyte Temperature of Aluminium Smelting Cells for Power Modulation, *Proceedings of the 41st International ICSOBA Conference*, Dubai, UAE, 5–9 November 2023, Paper AL55, *TRAVAUX* 52, 1799-1809.
26. Luning Ma et al., Model Predictive Control of Maintaining the Superheat of an Aluminium Smelting Cell during Power Modulation, *Proceedings of the 41st International ICSOBA Conference*, Dubai, UAE, 5–9 November 2023, Paper AL54, *TRAVAUX* 52, 1787-1797.
27. Ali Jassim et al., Studies on anode pre-heating using individual anode signals in Hall-Heroult reduction cells, *Light Metals* 2016, 623-628.
28. Zhuxian Qiu et al., Anodic Current Distribution and Current Efficiency of Aluminium Electrolysis Cells With Various Anode Settings, *ALUMINIUM*, Vol. 62, No. 7, (1986), 524-527.
29. A. Vallés, G. Aiquel, and R. Craig, Anode setting height optimisation, *Light Metals* 1991, 479-482.
30. Choon-Jie Wong et al., Modelling of Coupled Mass and Thermal Balances in Hall-Heroult Cells During Anode Change, *Journal of the Electrochemical Society*, Vol. 168, No. 21, (2021), 123506.
31. Choon-Jie Wong et al., Modeling Anode Current Pickup After Setting, *Light Metals* 2021, 351-358.
32. Gary P. Tarcy and K. Tørklep, Current efficiency in prebake and Søderberg cells, *Light Metals* 2005, 211-216.
33. Choon-Jie Wong et al., A Smart Individual Anode Current Measurement System and Its Applications, *Light Metals* 2023, 43-51.
34. Microchip Technology, SAM D/L/C - Oversampling and decimation feature, 2019, https://microchipsupport.force.com/s/article/SAM-D-L-C---Oversampling-and-decimation-feature.
35. Serge Despinasse and Eric Norel, Crane Electrical Insulation Monitoring in Potlines New CANDI™ 4.0 Development, *Light Metals* 2017, 715-721.
36. Vincent Delcourt et al., SMARTCrane, a Fives' Digital Solution for Aluminium Production Optimization, *Light Metals* 2024, 568-576.
37. Bibhudatta Mohanty et al., Networking and Centralized Monitoring Station of Pot Tending Assembly, *Proceedings of 36th International ICSOBA Conference*, Belém, Brazil, 29 October–1 November 2018, Paper AL27, *TRAVAUX* 47, 901-912.
38. Evan Andrews et al., Process Recovery to Unlock Power Efficiency Improvement at BSL, *Light Metals* 2023, 31-42.
39. Camila R. Silva et al., New 32-H Metal Tapping Cycle Implementation at ALBRAS, *Light Metals* 2024 508-513.
40. Choon-Jie Wong et al., Monitoring Cell Conditions and Anode Freeze Dissolution with Model-Based Soft Sensor After Anode Change, *Light Metals* 2023, 87-94.